International Journal of Multiphase Flow 64 (2014) 35–43

Contents lists available at ScienceDirect

International Journal of Multiphase Flow

journal homepage: www.elsevier.com/locate/ijmulflow

Toward numerical modeling of fine particle suspension using a two-way coupled Euler–Euler model. Part 1: Theoretical formulation and implications

Yi-Ju Chou [a,*], Fu-Chun Wu [b], Wu-Rong Shih [b]

[a] Institute of Applied Mechanics, National Taiwan University, Taipei 106, Taiwan
[b] Department of Bioenvironmental Systems Engineering, National Taiwan University, Taipei 106, Taiwan

ARTICLE INFO

Article history:
Available online 10 January 2014

Keywords:
Sediment suspension
Two-phase flow
Euler–Euler model

ABSTRACT

This paper presents a two-way coupled Euler–Euler model to simulate the dilute suspension of fine particles. The goal is to develop a three-dimensional numerical model that is capable of replicating detailed features of particle-laden turbulent flow. In addition to the terms found in typical two-phase Euler–Euler models, the present formulation also accounts for the effects of added mass and pressure, which are crucial to solid–liquid systems in which densities for each phase are of the same order. This study derives various approximations with which to assess existing model formulations, namely solid–gas equations, equilibrium-state approximation, simplified Euler models, and hindered settling velocity. We then emphasize the deviation of the present simulation results from the equilibrium state, which is simulated by the single-phase approach. We investigate simple examples of the Rayleigh–Taylor instability induced by the suspension of fine particles, the results of which reveals the distribution of non-equilibrium particle inertia. We then examine its influence on the carrier flow. A comparison between the present two-phase model and single-phase approximation demonstrates the importance of the coupled pressure on the evolution of a single bubble induced by the particle-driven Rayleigh Taylor instability.

1. Introduction

The suspension of fine sediment is an important geophysical phenomenon with critical implications for geological sciences, engineering practices in coastal regions, and countless hydrology-related applications. An important example is the under-water gravity current that is driven by the suspension of fine sediment (O(1–10 μm)), which plays a crucial role in erosion, sedimentation, and transport processes in coastal oceans and lakes. Recently, considerable attention has been paid to the numerical simulation of various issues related to sediment transport, including turbulence-induced suspensions (Zedler and Street, 2001; Zedler and Street, 2006; Chou and Fringer, 2008; Ozdemir et al., 2010), bed form dynamics (Chou et al., 2010), and turbidity currents (Necker et al., 2002; Necker et al., 2006; Cantero et al., 2009). These studies apply the scalar-limit and equilibrium conditions in which the transport of sediment is modeled using the scalar transport equation along with a constant settling velocity. This numerical approach, also called the single-phase Eulerian method, disregards the volumes occupied by particles as well as temporal and spatial variations in inter-phase interactions (e.g. particle drag). According to forces exerted on individual particles, this approach reveals zero-order quantities in terms of particle size (Nielsen, 1992). The single-phase approach is the standard approach when dealing with small particles in engineering and scientific problems. The convenience of the single-phase approach simplifies the incorporation of the suspended sediment transport model into the sophisticated Navier–Stokes flow solver, in particular the spectral-type flow solver. Thus, researchers have focused on employing the direct numerical simulation along with the scalar-limit sediment transport model to study particle-driven density currents (e.g. Necker et al., 2002; Necker et al., 2006; Cantero et al., 2008; Cantero et al., 2008; Cantero et al., 2009; Ozdemir et al., 2010). However, the underlying assumptions associated with single-phase approximation limit its applicability to actual flow problems. As pointed out in review articles of the dispersed two-phase flow system (Elghobashi, 1994; Balachandar and Eaton, 2010), the single-phase approach is applicable only to suspension problems in which the volumetric concentration $\phi \leqslant O(10^{-3})$ and the Stokes number, defined as the ratio of the particle relaxation time (τ_p) to the Kolmogorov time scale (τ_k), is $\leqslant 0.2$. This poses considerable limitations on the applicability of the single-phase method, with regard to problems in which ϕ can easily exceed 10^{-3} and turbulent intensity is strong (i.e. small τ_k). For example, under typical environmental conditions, field measurements have demonstrated that the concentration threshold of suspended sediment forming underwater particle-driven density currents in estuaries ranges

* Corresponding author. Tel.: +886 2 33665068.
E-mail address: yjchou@iam.ntu.edu.tw (Y.-J. Chou).

0301-9322/$ - see front matter © 2014 Elsevier Ltd. All rights reserved.
http://dx.doi.org/10.1016/j.ijmultiphaseflow.2013.12.008

from $\phi = 1.3 \times 10^{-2}$ to 1.7×10^{-2} (Mulder and Syvitski, 1995), which far exceeds the range in which the single-phase approximation applies. However, in practice, parameterization has enabled the application of the single-phase approach to problems of $\phi \sim 10^{-2}$. For example, (Snyder and Hsu, 2011) carry out two-dimensional Reynolds averaged Navier–Stokes (RANS) simulations to investigate convective sedimentation with ϕ ranging from 2.26×10^{-4} to 1.36×10^{-2}. These studies are meant to reveal large-scale features, while disregarding fine-scale details such as turbulence-particle interactions.

In order to gain a better understanding of the details associated with particle dynamics in turbulent flow, researchers have also simulated the motions of particles in turbulent flow fields by tracking individual particles according to their inertia (e.g. Elghobashi and Truesdell, 1993; Wang and Maxey, 1993; Yang and Lei, 1998; Dorgan and Loth, 2004; Bosse et al., 2006), a solution known as the Euler–Lagrange (EL) method. Nonetheless, the EL method is impractical for the study of sediment transport problems at scales of interest, in which a huge quantities of particles must be tracked. The prevalence of this problem in industrial applications has led to a number of recent studies focusing on the modeling of particle-laden flows using the Eulerian approach, as a mean to solve the averaged momentum of groups of particles (Riber et al., 2009). The resulting numerical framework, referred to as the Euler–Euler (EE) method, becomes a two-phase flow system in which the dispersed (particulate) phase is subject to inter-phase drag and gravity. The EE method resolves macro-scale particle dynamics in which the unresolved fluctuations are either disregarded or modeled using a Smagorinsky-type diffusion model. Compared to the EL method, the EE method produces satisfactory results with far greater efficiency for the study of particle-laden turbulent flows. Both EL and EE methods belong to the two-phase approach in which the particle inertia needs to be solved in addition to the momentum of the carrier flow field. A comprehensive derivation of different approximations of particle inertia based on different hydrodynamic forces exerted on a single particle has been discussed in detail in Ferry and Balachandar (2001). Numerical studies on particle-laden turbulence have focused on solid–gas dynamics, in which only particle drag and gravity contribute to particle inertia, while other terms such as added mass, lift, and Basset history terms are neglected. Except for added mass, the underlying rationality is the fact that these are high-order quantities in terms of particle size. The added mass can be disregarded only if the solid-flow density ratio is large, which is true for solid suspensions in gaseous flow in which solid–gas density ratio = $O(1000)$. However, this condition does not apply to solid–liquid mixtures, such as sediment transport, in which solid–liquid density ratio = $O(1)$.

During the past two decades, the two-phase EE method has been applied to problems of sediment transport. The formulation is based on the two-phase model proposed by Drew (1983), in which the momentum and mass transport of both phases are fully coupled. Along with a two-phase k—ϵ model for turbulence closure, (Hsu et al., 2003) applies the two-phase model to study steady-state sediment transport in the open channel flow. Their model is further applied to study the sheet flow condition in near-wall regions (Hsu et al., 2003) and the effect of the Schmidt number (Amoudry et al., 2005) on dilute sediment transport. Similar formulas with somehow different sediment parameters have been extensively applied to study steady-state sediment suspension in open channel flow, with special focuses on the validation against the experimental and analytical results as well as the validity of the turbulence model (e.g. Greimann and Holly, 2001, 2010, 2011). By simplifying governing equations into one- or two-dimensional momentum and mass transport equations, these studies demonstrate the efficacy of the two-phase flow model in revealing time-averaged concentration profiles in idealized laboratory settings without the ability to resolve detailed flow structures. Perhaps because the formulation originated with solid–gas systems, the effect of added mass was disregarded. Thus, there remains a need for the development of a three-dimensional numerical flow solver capable of revealing, in detail, the turbulent features of sediment-laden flows.

A different EE modeling approach is presented in Cantero et al. (2008), in which the result derived in Ferry and Balachandar (2001) is employed to reformulate an EE model to study turbidity currents in two-dimensional settings. By introducing an additional first order quantity, namely $\tau_p D\mathbf{u}/Dt$ in which $\mathbf{u}$ is the fluid velocity and D/Dt is the material derivative, the simulation results in Cantero et al. (2008) reveal important features induced by the non-equilibrium particle inertia (e.g. preferential accumulation) and its effect on the current dynamics. Because the particle inertia is described as an explicit function of the continuous-phase momentum, the model presented in Cantero et al. (2008) retains the computational efficiency of the single-phase method without solving the additional momentum equations for the particle phase. Because the continuous-phase momentum is solved under the equilibrium-state and scalar-limit assumptions, the spectral-type Navier–Stokes solver is employed to solve the flow field. Moreover, based on Ferry and Balachandar (2001), the effect of the added mass is first considered in the formulation of the particle relaxation time.

This study first outlines the general Euler–Euler two-fluid model for the simulation of the suspension of particles. We then relate the present formulation to four special cases. The first case is the solid–gas system. While such a system has been extensively studied in the context of dispersed two-phase flows, it is important to examine how this system differs from the solid–liquid system and to assess the applicability of the resulting model to sediment transport problems. The second case is the equilibrium-state approximation, in which we highlight the buoyant effect induced by particles in the single-phase formulation, which has been extensively employed to model suspended sediment transport in various scales. In the third case, the deviation of particle inertia from the equilibrium state is taken into account. Disregarding any particle feedback other than the buoyant effect in the continuous phase, this leads to a simplified EE model presented in Cantero et al. (2008). In the fourth case, through the simple derivation, we obtain the reduction of the settling velocity during hindered settling, which demonstrates the importance of pressure coupling in modeling sediment suspensions. Through the discussion of the four special cases, we examine current approximations and parameters that have been extensively employed in the context of sediment transport problems. This would provide useful insights into the development of sediment transport models at different levels of complexity.

The rest of this paper is organized as follows. In Section 2, we establish the setting of the present problems and derive the mathematical formulations. In Section 3, important approximations are derived from the present two-phase formulation, and current formulas are justified. In Section 4, we discuss the effects arising from particle inertia and mixture incompressibility using simple numerical examples of the particle-induced Rayleigh–Taylor instability for illustration. Conclusion are drawn in Section 5.

2. Mathematical formulation

2.1. Statement of the problem

Deriving the Euler–Euler equations for the two-phase dispersed system requires setting the following important conditions:

- *Small particle size:* Particle size is assumed to be small enough to ensure that the particle relaxation time (τ_p) is less than the Kolmogorov time scale (τ_K) of the flow field. Thus, no crossing of particle trajectories is considered, and the particle velocity field is unique. If this condition is not satisfied, a probability density function (PDF) approach based on a conditional ensemble average can be applied (Fevrier et al., 2005). In such a case, the contribution to the dispersed momentum from the random uncorrelated velocity of particles must be considered in the Eulerian approach (Fevrier et al., 2005; Riber et al., 2009). To justify the condition of the unique particle flow field, one can estimate the particle relaxation time under the assumption of the Stokes flow,

$$\tau_p = \frac{\rho_p d_p^2}{18\mu}, \tag{1}$$

where ρ_p is the particle density, d_p is the particle diameter, and μ is the viscosity of the carrier flow. For example, for the fine suspensions considered in this study, we are interested in the particle size of $O(10\ \mu m)$ suspended in waters. Using $\rho_p = 2650$ kg m^{-3} ,$\mu = 1002$ Pa s, and $d_p = 10\ \mu m$, the relaxation time $\tau_p \approx 1.5 \times 10^{-5}$ s. Even with a larger particle size, $d_p = 100\ \mu m$, $\tau_p \approx 1.5 \times 10^{-3}$ s. Therefore, as long as $\tau_K > O(10^{-3}\ s)$, the deterministic Eulerian approach provides a valid approximation for describing the motion of particles in the problems addressed in this study, i.e. fine particles suspended in waters. However, considering the case of a solid–gas system, the condition is somewhat more restrictive. For example, for the aforementioned small particle size $d_p = 10\ \mu m$, using the atmospheric viscosity $\mu = 1.8 \times 10^{-5}$ Pa s results in $\tau_p \approx 8.2 \times 10^{-4}$ s, while $d_p = 100\ \mu m$ leads to $\tau_p \approx 8.2 \times 10^{-2}$ s, and the limit for τ_K for which the Eulerian model can be applied is much more restrictive than in the solid–liquid system. This demonstrates the need to describe the motion of particles using the PDF approach or Lagrangian point-particle tracking method. Moreover, although the PDF and point-particle approaches provide a more accurate description of the motion of particles, describing the feedback forces from the particulate phase to the carrier phase can be a daunting task. In order to formulate the fully two-way coupled equations, which is particularly important for solid–liquid systems, this study focuses on particles with a small relaxation time to ensure the applicability of the Eulerian model.
- *Dilute suspension:* The condition stipulating a small volumetric concentration (ϕ) of the dispersed particulate phase must also be satisfied in order to avoid the need to consider particle–particle interactions. It has been well documented that in terms of particulate stress resulting from collisions and friction, $\phi < 10^{-3}$ is considered dilute; therefore, either one- or two-way coupled approaches can be applied, while for dense suspensions, $\phi > 10^{-3}$, a four-way coupled approach is required (Elghobashi, 1994; Balachandar and Eaton, 2010). In applications involving environmental flow (e.g. sediment suspension), this stringent restriction is usually relaxed and the Eulerian model is applied to the case of $\phi = O(10^{-2})$ without considering interactions among particulate matter. For further justification, we can examine the Bagnold number, which characterizes the ratio of grain collision stress to fluid viscous stress. The Bagnold number (Ba) is defined as

$$Ba = \frac{\rho_p d_p^2 \lambda^{\frac{1}{2}} \gamma}{\mu}, \tag{2}$$

where γ is the shear rate and λ is the linear concentration, given by

$$\lambda = \frac{1}{\left(\frac{\phi_{pk}}{\phi}\right)^{\frac{1}{3}} - 1}, \tag{3}$$

where ϕ_{pk} is the close packing concentration, usually ranging from 0.4 to 0.6. For $Ba < 40$, viscous fluid stresses dominate collision stresses in the solid–fluid mixture; otherwise, collision stresses dominate. For the suspension of solids in water, if $\phi_{d,pk} = 0.5$ and we consider an extreme case of $d_p = 100\ \mu m$, $\phi = 0.01, Ba$ remains far below unity unless γ is unrealistically large (i.e. $O(10^3\ s^{-1})$). However, the condition of a small Ba can be violated using the same concentration and properties of particles in the solid–gas system when the shear rate is reasonably large (i.e. $O(10\ s^{-1})$), due to the low density of the gas.

In summary, under the conditions of small particle size and dilute suspension, the Eulerian approach is suitable for describing the motion of particles in fluid. Moreover, the above arguments outline the advantage of treating suspended particles in flowing liquid as a continuum as opposed to a gaseous flow because the motion of particles heavily depends on the flow field. This is mainly because densities vary considerably in liquids and gases, resulting in discrepancies between solid–fluid density ratios of the solid–gas systems ($\rho_p/\rho_g \approx O(1000)$) and solid–liquid systems ($\rho_p/\rho_g \approx O(1)$). Despite the fact that the method simplifies the problem, the effect of inter-phase momentum exchange is more pronounced in solid–liquid systems than in solid–gas systems.

2.2. Fully-coupled two-phase equations

Beginning from the general mathematical formulation for a two-phase system describing incompressible flow, the averaged governing equations read (Drew and Passman, 1998)

$$\frac{\partial \phi_d}{\partial t} + \nabla \cdot (\bar{\mathbf{u}}_d \phi_d) = 0, \tag{4}$$

$$\frac{\partial \phi_c}{\partial t} + \nabla \cdot (\bar{\mathbf{u}}_c \phi_c) = 0, \tag{5}$$

$$\frac{\partial \phi_d \rho_d \bar{\mathbf{u}}_d}{\partial t} + \nabla \cdot [\bar{\mathbf{u}}_d (\phi_d \rho_d \bar{\mathbf{u}}_d)] = -\phi_d \rho_c \nabla \bar{p} + \phi_d \rho_d \mathbf{M}_{cd} + \phi_d (\rho_d - \rho_c)\mathbf{g} - \nabla \cdot \left(\phi_d \rho_d \overline{\mathbf{\Sigma}}_{Re,d}\right), \tag{6}$$

$$\frac{\partial \phi_c \rho_c \bar{\mathbf{u}}_c}{\partial t} + \nabla \cdot [\bar{\mathbf{u}}_c (\phi_c \rho_c \bar{\mathbf{u}}_c)] = -\phi_c \rho_c \nabla \bar{p} - \phi_d \rho_d \mathbf{M}_{cd} - \nabla \cdot \left(\phi_c \rho_c \overline{\mathbf{\Sigma}}_{Re,c}\right) + \nabla \cdot \rho_c \overline{\mathbf{\Sigma}}_{vis}, \tag{7}$$

where subscripts d and c indicate dispersed phase and continuous phase, respectively, ϕ is volume fraction ($\phi_d + \phi_c = 1$), $\mathbf{u}$ is the velocity vector, p is the dynamic pressure, $\mathbf{M}_{cd}$ is the inter-phase momentum exchange, ρ_d is the density of the dispersed phase, ρ_c is the density of the continuous phase, g is gravity, $\overline{\mathbf{\Sigma}}_{Re}$ is the Reynolds stress arising from spatial variation in the sub-grid scale, and $\overline{\mathbf{\Sigma}}_{vis}$ is the viscous stress of the mixture. In the present study, we disregard any rheological change induced by fine particles, thus obtaining (Drew and Passman, 1998)

$$\overline{\mathbf{\Sigma}}_{vis} = \nu \left[\nabla \bar{\mathbf{u}}_m + (\nabla \bar{\mathbf{u}}_m)^{\mathrm{T}}\right], \tag{8}$$

where ν is the kinematic viscosity of clear water, and $\bar{\mathbf{u}}_m = \phi_c \bar{\mathbf{u}}_c + \phi_d \bar{\mathbf{u}}_d$ is the mixture velocity. We adopt the phase-average, denoted using the overbar, which is defined as

$$\bar{\beta} = \frac{\overline{\beta\phi}}{\phi}, \tag{9}$$

for any physical quantity β, assuming that it commutes for any differential operator (Drew and Passman, 1998). Eqs. (4)–(7) are standard formulations used in the modeling of two-phase flow systems. In the context of sediment suspension, they are usually simplified to form single-phase equations (Necker et al., 2002; Necker et al.,

2006; Cantero et al., 2009), simplified two-phase equations (Cantero et al., 2008; Cantero et al., 2008) or one- or two-dimensional vertical (1 or 2DV) models for analysis (Greimann and Holly, 2001; Hsu et al., 2003; Hsu et al., 2003; Jha and Bombardelli, 2010; Chen et al., 2011). Our aim in this study is to manipulate the above equations to develop a more precise three-dimensional model for the simulation of particle-laden flows with the less stringent limitations with regard to concentration.

Because ρ_d and ρ_c are constants, we can use the relation of mass balance given by Eqs. (4) and (5) and expand the viscosity term, in order to arrange Eqs. (6) and (7) as follows:

$$\phi_d\rho_d\left[\frac{\partial\bar{\mathbf{u}}_d}{\partial t}+\bar{\mathbf{u}}_d\cdot\nabla\bar{\mathbf{u}}_d\right]=-\phi_d\rho_c\nabla\bar{p}+\phi_d\rho_d\mathbf{M}_{cd}+\phi_d(\rho_d-\rho_c)\mathbf{g}-\nabla\cdot\left(\phi_d\rho_d\bar{\bar{\boldsymbol{\Sigma}}}_{Re,d}\right), \tag{10}$$

$$\begin{aligned}\phi_c\rho_c\left[\frac{\partial\bar{\mathbf{u}}_c}{\partial t}+\bar{\mathbf{u}}_c\cdot\nabla\bar{\mathbf{u}}_c\right]&=-\phi_c\rho_c\nabla\bar{p}-\phi_d\rho_d\mathbf{M}_{cd}-\nabla\cdot\left(\phi_c\rho_c\bar{\bar{\boldsymbol{\Sigma}}}_{Re,c}\right)\\&\quad+\phi_c\rho_c\nu\nabla^2\bar{\mathbf{u}}_c+\phi_d\rho_d\nu\nabla^2\bar{\mathbf{u}}_d\\&\quad+2\rho_d\nabla\phi_d\cdot\nu\nabla(\bar{\mathbf{u}}_d-\bar{\mathbf{u}}_c)\\&\quad+\rho_d\nabla^2\phi_d\cdot\nu(\bar{\mathbf{u}}_d-\bar{\mathbf{u}}_c).\end{aligned} \tag{11}$$

In order to obtain the inter-phase momentum exchange term, we begin from the description of motion of a particle. Momentum contributions to particle inertia arise from the pressure gradient of the carrier flow, gravitational force, and the inter-phase momentum exchanges that are functions of the velocity difference between the flow and the particle. Using the Auton's form for the added mass (Auton et al., 1988), the inter-phase momentum exchanges can be further divided into two parts. The first part is the added mass effect that is a function of flow acceleration, $D\mathbf{u}_c/Dt - d\mathbf{u}_p/dt$, in which $D/Dt=\partial/\partial t+\mathbf{u}_c\cdot\nabla$ and $d/dt=\partial/\partial t+\mathbf{u}_p\cdot\nabla$ represent material derivatives with respect to the flow and particle, respectively. The second part comprises the Stokes drag, Basset history term, and Saffman lift, all of which depend on the local velocity difference, $\mathbf{u}_c-\mathbf{u}_p$. Thus, denoting the second part of the inter-phase momentum exchanges as $\mathbf{F}(\mathbf{u}_c-\mathbf{u}_p)$, the formula to describe motion of the individual particle with mass m_p takes the following form (Ferry and Balachandar, 2001):

$$m_p\frac{d\mathbf{u}_p}{dt}=-m_c\nabla p+(m_p-m_c)\mathbf{g}+C_{vm}m_c\left(\frac{D\mathbf{u}_c}{Dt}-\frac{d\mathbf{u}_p}{dt}\right)+\mathbf{F}(\mathbf{u}_c-\mathbf{u}_p), \tag{12}$$

and

$$\mathbf{F}(\mathbf{u}_c-\mathbf{u}_p)=6\pi d_p\mu(\mathbf{u}_c-\mathbf{u}_p)+6\pi d_p^2\mu\left[\int_0^t\frac{\mathbf{u}_c'(\xi)-\mathbf{u}_p'(\xi)}{\sqrt{\nu\pi(t-\xi)}}d\xi\right]+\frac{9J_\infty}{\pi}d_p^2\sqrt{\frac{\mu\rho_c}{|\omega|}}(\mathbf{u}_c-\mathbf{u}_p)\times\omega, \tag{13}$$

where the first term in RHS is the Stokes drag, the second term is the Basset history term, and the third term is the Saffman lift force (Saffman, 1965), in which J_∞ is the coefficient for the Saffman lift force, and ω is the vorticity of the external flow field surrounding a particle. Next, we take the averaged motion of n particles in a control volume using the relationship obtained from Eq. (9), such that $n\bar{\mathbf{u}}_d=\overline{n\mathbf{u}}_d=\sum_{i=1}^n\mathbf{u}_{p,i}$, and introduce $\mathcal{F}$ to describe the phase-averaged inter-phase momentum exchange as

$$\frac{1}{n}\sum_{i=1}^n\mathbf{F}(\mathbf{u}_{c,i}-\mathbf{u}_{p,i})=\mathcal{F}(\bar{\mathbf{u}}_c-\bar{\mathbf{u}}_d)+f', \tag{14}$$

where the fluctuation term f' arises from the non-linear inter-phase momentum exchange. It can be thus determined from Eqs. (12) and (14) that the inter-phase momentum exchange can be described as follows:

$$\mathbf{M}_{cd}=\mathcal{F}(\bar{\mathbf{u}}_c-\bar{\mathbf{u}}_d)+f'+C_{vm}\times\frac{\rho_c}{\rho_d}\left[\frac{\partial\bar{\mathbf{u}}_c}{\partial t}+\bar{\mathbf{u}}_c\cdot\nabla\bar{\mathbf{u}}_c-\frac{\partial\bar{\mathbf{u}}_d}{\partial t}-\bar{\mathbf{u}}_d\cdot\nabla\bar{\mathbf{u}}_d+\nabla\cdot\left(\bar{\bar{\boldsymbol{\Sigma}}}_{Re,c}-\bar{\bar{\boldsymbol{\Sigma}}}_{Re,d}\right)\right], \tag{15}$$

where the third term on RHS represents the contribution from added mass.

Taking $\phi=\phi_d$ and $\phi_c=1-\phi_d=1-\phi$, substitution of Eq. (15) into Eqs. (10) and (11) leads to

$$\begin{aligned}&\left(1+\frac{C_{vm}}{s}\right)\left[\frac{\partial\bar{\mathbf{u}}_d}{\partial t}+\bar{\mathbf{u}}_d\cdot\nabla\bar{\mathbf{u}}_d\right]-\frac{C_{vm}}{s}\left[\frac{\partial\bar{\mathbf{u}}_c}{\partial t}+\bar{\mathbf{u}}_c\cdot\nabla\bar{\mathbf{u}}_c\right]\\&=\mathcal{F}(\bar{\mathbf{u}}_c-\bar{\mathbf{u}}_d)+f'-\frac{\nabla\bar{p}}{s}+\mathbf{g}'-\frac{1}{\phi}\nabla\cdot\left(\phi\bar{\bar{\boldsymbol{\Sigma}}}_{Re,d}\right)+\frac{C_{vm}}{s}\nabla\cdot\left(\bar{\bar{\boldsymbol{\Sigma}}}_{Re,c}-\bar{\bar{\boldsymbol{\Sigma}}}_{Re,d}\right),\end{aligned} \tag{16}$$

$$\begin{aligned}&-C_{vm}\frac{\phi}{1-\phi}\left[\frac{\partial\bar{\mathbf{u}}_d}{\partial t}+\bar{\mathbf{u}}_d\cdot\nabla\bar{\mathbf{u}}_d\right]+\left(1+C_{vm}\frac{\phi}{1-\phi}\right)\left[\frac{\partial\bar{\mathbf{u}}_c}{\partial t}+\bar{\mathbf{u}}_c\cdot\nabla\bar{\mathbf{u}}_c\right]\\&=-\frac{\phi}{1-\phi}s\mathcal{F}(\bar{\mathbf{u}}_c-\bar{\mathbf{u}}_d)-\frac{\phi}{1-\phi}sf'-\nabla\bar{p}-\frac{1}{1-\phi}\nabla\cdot\left[(1-\phi)\bar{\bar{\boldsymbol{\Sigma}}}_{Re,c}\right]-C_{vm}\frac{\phi}{1-\phi}\nabla\cdot\left(\bar{\bar{\boldsymbol{\Sigma}}}_{Re,c}-\bar{\bar{\boldsymbol{\Sigma}}}_{Re,d}\right)\\&\quad+\frac{\phi}{1-\phi}\nu\nabla^2\bar{\mathbf{u}}_d+\nu\nabla^2\bar{\mathbf{u}}_c+2\frac{\nabla\phi}{1-\phi}\cdot\nu\nabla(\bar{\mathbf{u}}_d-\bar{\mathbf{u}}_c)+\frac{\nabla^2\phi}{1-\phi}\cdot\nu(\bar{\mathbf{u}}_d-\bar{\mathbf{u}}_c).\end{aligned} \tag{17}$$

where $s=\rho_d/\rho_c$ is the density ratio and $\mathbf{g}'=\mathbf{g}(s-1)/s$. Eqs. (10) and (11) can be rewritten as a coupled two-phase system as follows:

$$\begin{aligned}&\begin{bmatrix}1+\frac{C_{vm}}{s}&-\frac{C_{vm}}{s}\\-C_{vm}\frac{\phi}{1-\phi}&1+C_{vm}\frac{\phi}{1-\phi}\end{bmatrix}\begin{bmatrix}\frac{\partial\bar{\mathbf{u}}_d}{\partial t}\\\frac{\partial\bar{\mathbf{u}}_c}{\partial t}\end{bmatrix}+\begin{bmatrix}1+\frac{C_{vm}}{s}&-\frac{C_{vm}}{s}\\-C_{vm}\frac{\phi}{1-\phi}&1+C_{vm}\frac{\phi}{1-\phi}\end{bmatrix}\begin{bmatrix}\bar{\mathbf{u}}_d\cdot\nabla\bar{\mathbf{u}}_d\\\bar{\mathbf{u}}_c\cdot\nabla\bar{\mathbf{u}}_c\end{bmatrix}\\&=\begin{bmatrix}\mathcal{F}(\bar{\mathbf{u}}_c-\bar{\mathbf{u}}_d)+f'+\mathbf{g}'\\-\frac{\phi}{1-\phi}s\mathcal{F}(\bar{\mathbf{u}}_c-\bar{\mathbf{u}}_d)-\frac{\phi}{1-\phi}sf'\end{bmatrix}+\begin{bmatrix}-\frac{\nabla\bar{p}}{s}\\-\nabla\bar{p}\end{bmatrix}\\&\quad+\begin{bmatrix}0\\\frac{\phi}{1-\phi}\nu\nabla^2\bar{\mathbf{u}}_d+\nu\nabla^2\bar{\mathbf{u}}_c+2\frac{\nabla\phi}{1-\phi}\cdot\nu\nabla(\bar{\mathbf{u}}_d-\bar{\mathbf{u}}_c)+\frac{\nabla^2\phi}{1-\phi}\cdot\nu(\bar{\mathbf{u}}_d-\bar{\mathbf{u}}_c)\end{bmatrix}\\&\quad-\begin{bmatrix}1+\frac{C_{vm}}{s}&-\frac{C_{vm}}{s}\\-C_{vm}\frac{\phi}{1-\phi}&1+C_{vm}\frac{\phi}{1-\phi}\end{bmatrix}\begin{bmatrix}\nabla\cdot\bar{\bar{\boldsymbol{\Sigma}}}_{Re,d}\\\nabla\cdot\bar{\bar{\boldsymbol{\Sigma}}}_{Re,c},\end{bmatrix}-\begin{bmatrix}\frac{\nabla\phi}{\phi}\cdot\bar{\bar{\boldsymbol{\Sigma}}}_{Re,d}\\\frac{\nabla(1-\phi)}{1-\phi}\cdot\bar{\bar{\boldsymbol{\Sigma}}}_{Re,c}.\end{bmatrix}.\end{aligned} \tag{18}$$

For problems involving the suspension of fine sediment, we focus on particles of small size, $d_p\approx O(10\ \mu\text{m})$, and are concerned only with the bulk properties of the sediment–water mixture. Therefore, the $O\left(d_p^2\right)$ quantities in inter-phase momentum transfer (Eq. (13)), such as the lift force and Basset history term, are disregarded. Here, we use the conventional formulation of particle drag to represent the inter-phase momentum exchange due to relative velocity, i.e.

$$\mathcal{F}(\bar{\mathbf{u}}_c-\bar{\mathbf{u}}_d)=\frac{\bar{\mathbf{u}}_c-\bar{\mathbf{u}}_d}{\tau_p}. \tag{19}$$

Disregarding the inter-phase fluctuation term ($f'=0$) and using Eq. (19), Eq. (18) can once again be written as follows:

$$\begin{bmatrix}\frac{\partial\bar{\mathbf{u}}_d}{\partial t}\\ \frac{\partial\bar{\mathbf{u}}_c}{\partial t}\end{bmatrix}+\begin{bmatrix}\bar{\mathbf{u}}_d\cdot\nabla\bar{\mathbf{u}}_d\\ \bar{\mathbf{u}}_c\cdot\nabla\bar{\mathbf{u}}_c\end{bmatrix}=\mathcal{A}\begin{bmatrix}\frac{\bar{\mathbf{u}}_c-\bar{\mathbf{u}}_d}{\tau_p}\\ -\frac{\phi}{1-\phi}s\frac{\bar{\mathbf{u}}_c-\bar{\mathbf{u}}_d}{\tau_p}\end{bmatrix}+\mathcal{A}\begin{bmatrix}\mathbf{g}'\\ 0\end{bmatrix}+\mathcal{A}\begin{bmatrix}-\frac{\nabla\bar{p}}{s}\\ -\nabla\bar{p}\end{bmatrix}+\mathcal{A}\begin{bmatrix}0\\ \frac{\phi}{1-\phi}\nu\nabla^2\bar{\mathbf{u}}_d+\nu\nabla^2\bar{\mathbf{u}}_c+2\frac{\nabla\phi}{1-\phi}\cdot\nu\nabla(\bar{\mathbf{u}}_d-\bar{\mathbf{u}}_c)+\frac{\nabla^2\phi}{1-\phi}\nu(\bar{\mathbf{u}}_d-\bar{\mathbf{u}}_c)\end{bmatrix}-\begin{bmatrix}\nabla\cdot\bar{\boldsymbol{\Sigma}}_{Re,d}\\ \nabla\cdot\bar{\boldsymbol{\Sigma}}_{Re,c}\end{bmatrix}-\mathcal{A}\begin{bmatrix}\frac{\nabla\phi}{\phi}\cdot\bar{\boldsymbol{\Sigma}}_{Re,d}\\ \frac{\nabla(1-\phi)}{1-\phi}\cdot\bar{\boldsymbol{\Sigma}}_{Re,c}\end{bmatrix},\tag{20}$$

where

$$\mathcal{A}=\begin{bmatrix}1+\frac{C_{vm}}{s} & -\frac{C_{vm}}{s}\\ -C_{vm}\frac{\phi}{1-\phi} & 1+C_{vm}\frac{\phi}{1-\phi}\end{bmatrix}^{-1}=\frac{1}{1+\frac{C_{vm}}{s}+C_{vm}\frac{\phi}{1-\phi}}\times\begin{bmatrix}1+C_{vm}\frac{\phi}{1-\phi} & \frac{C_{vm}}{s}\\ C_{vm}\frac{\phi}{1-\phi} & 1+\frac{C_{vm}}{s}\end{bmatrix},\tag{21}$$

is a matrix that determines the partition of the momentum source/sink from one phase to the other due to the effect of added mass. Eq. (20) is the final coupled formulation for the numerical simulation of fine particle suspensions in this study. In addition to the inter-phase drag term, which has appeared in many previous studies, the present formulation includes added mass and enables coupling through pressure. The added mass effect can be accounted for through the inversion of the matrix to form partition matrix $\mathcal{A}$ (see Eq. (21)), which calculates the partitioning of each momentum source from one phase into the other. The upper off-diagonal component of $\mathcal{A}$ shows that as density ratio (s) increases, the added mass effect from the carrier flow to the solid phase decreases. A typical example would be $s\sim O(1000)$ with solids suspended in a gaseous flow, such that the added mass effect from flow to solid can be eliminated, as discussed in Section 3.1. On the other hand, the lower off-diagonal component of the partition matrix $\mathcal{A}$ shows that the added mass effect from the solid to the fluid phase depends on the volume concentration of the solid phase; i.e. partitioning of the momentum source from the solid to fluid phase increases with an increase in concentration. Therefore, in a very dilute suspension, the added mass effect in the carrier flow phase can be disregarded. A number of important approximations are discussed in the following section.

3. Special approximations

3.1. Case 1: Solid–gas system

As density ratio s is large, such as $s\approx 1000$ in the solid–gas system, all terms in Eq. (20) associated with the reciprocal of s becomes negligible. This enables partition matrix $\mathcal{A}_{sg}$ to be simplified from $\mathcal{A}$ and written as follows:

$$\mathcal{A}_{sg}=\frac{1}{1+C_{vm}\frac{\phi}{1-\phi}}\begin{bmatrix}1+C_{vm}\frac{\phi}{1-\phi} & 0\\ C_{vm}\frac{\phi}{1-\phi} & 1\end{bmatrix},\tag{22}$$

and Eq. (20) can be reduced to

$$\frac{\partial}{\partial t}\begin{bmatrix}\bar{\mathbf{u}}_d\\ \bar{\mathbf{u}}_c\end{bmatrix}+\begin{bmatrix}\bar{\mathbf{u}}_d\cdot\nabla\bar{\mathbf{u}}_d\\ \bar{\mathbf{u}}_c\cdot\nabla\bar{\mathbf{u}}_c\end{bmatrix}=\begin{bmatrix}\frac{\bar{\mathbf{u}}_c-\bar{\mathbf{u}}_d}{\tau_p}\\ -\frac{\phi}{1-\phi}s\frac{\bar{\mathbf{u}}_c-\bar{\mathbf{u}}_d}{\tau_p}\end{bmatrix}+\begin{bmatrix}\mathbf{g}'\\ \mathcal{A}_{sg,(2,1)}\mathbf{g}'\end{bmatrix}+\begin{bmatrix}0\\ -\mathcal{A}_{sg,(2,2)}\nabla\bar{p}\end{bmatrix}+\begin{bmatrix}0\\ \mathcal{A}_{sg,(2,2)}\nu\nabla^2\bar{\mathbf{u}}_c\end{bmatrix}+\begin{bmatrix}0\\ \frac{\phi}{1-\phi}\mathcal{A}_{sg,(2,2)}\nu\nabla^2\bar{\mathbf{u}}_d\end{bmatrix}+\begin{bmatrix}0\\ \mathcal{A}_{sg,(2,2)}\frac{\nabla\phi}{1-\phi}\cdot\nu\nabla(\bar{\mathbf{u}}_d-\bar{\mathbf{u}}_c)-\mathcal{A}_{sg,(2,2)}\frac{\nabla^2\phi}{1-\phi}\nu(\bar{\mathbf{u}}_d-\bar{\mathbf{u}}_c)\end{bmatrix}-\begin{bmatrix}\nabla\cdot\bar{\Sigma}_{Re,d}\\ \nabla\cdot\bar{\Sigma}_{Re,c}\end{bmatrix}-\begin{bmatrix}\frac{\nabla\phi}{\phi}\cdot\bar{\Sigma}_{Re,d}\\ \mathcal{A}_{sg,(2,2)}\frac{\nabla\phi}{1-\phi}\cdot(\bar{\Sigma}_{Re,d}-\bar{\Sigma}_{Re,c})\end{bmatrix},\tag{23}$$

where we have also adopted the inequality, $s\gg C_{vm}$. According to Eq. (23), the influence of the two-way coupling on the dispersed phase is only through Stokes drag. It can be seen that coupling effects resulting from added mass vanish in the dispersed-phase momentum equation because of the large density ratio but remain in the continuous-phase momenturm equation, as a function of ϕ. Moreover, under very dilute conditions such that $\phi,\nabla\phi$, and $\nabla^2\phi$ are all much less than unity, the single-phase momentum equation of the incompressible flow is recovered. In such a case, the modeling approach is reduced to a two-phase formulation similar to the one-way coupled Euler–Lagrange approach, in which the motions of particles are induced by the combination of the Stokes drag and body force without exerting feedback to the carrier fluid. In the solid–gas system, this provides a good approximation of particle motion (i.e. independent of concentration) as long as the inter-particle stress is not a matter of concern. In contrast, for the continuous phase, added mass always appears with concentration. Only when the concentration is very dilute can the motion of the continuous phase be treated as a single-phase flow.

3.2. Case 2: Equilibrium-state approximation

In the case of a very small relaxation time relative to the time scale of interest, an important approximation can be obtained by assuming that particles precisely follow the flow field with the addition of a terminal velocity induced by gravity. That is, the gravitational force exerted on the particles is in balance with the drag on the surface of particles. This results in a terminal speed, which is the only relative velocity between two phases. Mathematically, this can be expressed as

$$\bar{\mathbf{u}}_d=\bar{\mathbf{u}}_c+w_{s,0}\hat{\mathbf{e}}_3,\tag{24}$$

where $w_{s,0}$ is the settling velocity of a single particle, which can be calculated by balancing Stokes drag and reduced gravity as follows:

$$\frac{\bar{\mathbf{u}}_c-\bar{\mathbf{u}}_d}{\tau_p}+\mathbf{g}'=0,\tag{25}$$

resulting in $w_{s,0}=-\tau_p g'$, which depends only on flow and properties of particles. Here we introduce a new momentum exchange term, $\mathbf{M}'_{cd}$, without Stokes drag as

$$\mathbf{M}'_{cd}\equiv\mathbf{M}_{cd}-\frac{\bar{\mathbf{u}}_c-\bar{\mathbf{u}}_d}{\tau_p}.\tag{26}$$

Neglecting all the Reynolds stress terms for simplicity and substituting Eqs. (24)–(26) into the original two-phase system, Eqs. (10) and (11), results in

$$\phi\rho_d\left[\frac{\partial\bar{\mathbf{u}}_c}{\partial t}+\bar{\mathbf{u}}_c\cdot\nabla\bar{\mathbf{u}}_c-w_{s,0}\frac{\partial\bar{\mathbf{u}}_c}{\partial z}\right]=-\phi\rho_c\nabla\bar{p}+\rho_d\phi\mathbf{M}'_{cd},\tag{27}$$

$$(1-\phi)\rho_c\left[\frac{\partial\bar{\mathbf{u}}_c}{\partial t}+\bar{\mathbf{u}}_c\cdot\nabla\bar{\mathbf{u}}_c\right]=-(1-\phi)\rho_c\nabla\bar{p}-\rho_d\phi(\mathbf{M}'_{cd}-\mathbf{g}')+\nabla\cdot\bar{\boldsymbol{\Sigma}}_{vis},\tag{28}$$

in which $\bar{\boldsymbol{\Sigma}}_{vis}$ represents the bulk viscous stress given by Eq. (8). Summing Eqs. (27) and (28) and using the mixture density defined as

$$\rho=\phi\rho_d+\phi_c\rho_c=\phi\rho_d+(1-\phi)\rho_c,\tag{29}$$

leads to

$$\frac{\partial\bar{\mathbf{u}}_c}{\partial t}+\bar{\mathbf{u}}_c\cdot\nabla\bar{\mathbf{u}}_c-\frac{\phi\rho_d}{\rho}w_{s,0}\cdot\frac{\partial\bar{\mathbf{u}}_c}{\partial z}=-\frac{\rho_c}{\rho}\nabla\bar{p}+\frac{\phi\rho_d}{\rho}\mathbf{g}'+\frac{1}{\rho}\nabla\cdot\bar{\boldsymbol{\Sigma}}_{vis}.\tag{30}$$

In the case of very dilute suspension (e.g. $\phi<1\%$), one can assume that $\rho\approx\rho_c$ and $\phi\rho_d w_{s,0}/\rho\ll\bar{u}_c$ for small particles. Eq. (30) can be further simplified to

$$\frac{\partial \bar{\mathbf{u}}_c}{\partial t} + \bar{\mathbf{u}}_c \cdot \nabla \bar{\mathbf{u}}_c = -\nabla \bar{p} + \phi s \mathbf{g}' + \nu \nabla^2 \bar{\mathbf{u}}_c. \tag{31}$$

The motion of particles can thus be described as a transport equation of a concentration field,

$$\frac{\partial \phi}{\partial t} + \nabla \cdot (\bar{\mathbf{u}}_c \phi) - \frac{\partial}{\partial z}(w_s \phi) = 0. \tag{32}$$

For dilute suspensions, one can readily disregard the volume occupied by particles, such that incompressibility is applied only to the continuous phase; i.e.

$$\nabla \cdot \bar{\mathbf{u}}_c = 0. \tag{33}$$

Eqs. (31)–(33) are referred to as the single-phase method, which has been widely used to study sediment suspension problems. This convenient approach requires that one solves only the momentum equations for the continuous phase with sediment-induced effective density stratification.

According to the above derivation, it should be mentioned that the single-phase model used to describe flow motion using the original momentum equation along with a stratification term can only be obtained by combining the momentum equations of two phases (i.e. the mixture). As a result, we first obtain Eq. (30) before assuming that the concentration is dilute in order to obtain Eq. (31). Ignoring changes in the flow rheology as well as non-Boussinesq pressure, one difference between Eqs. (30) and (31) is the third term on LHS, which is an additional vertical convection induced by the settling of particles. Another difference is the coefficient $\phi\rho_d/\rho$, which appears in both the settling-induced convective term as well as the buoyancy term. In comparison to the buoyancy term in Eq. (31), total density (ρ) in the denominator makes the body force weaker in Eq. (30) than it appears in the commonly-used formulation (Eq. (31)) with an increase in ϕ. This is a more reasonable approach because as the mixture density of the ambient flow increases, the vertical acceleration of sedimentation should be less than that observed in a clear water column. The same analogy can also be applied to the term of settling induced convection.

In practice, the two-phase flow model is not an appealing strategy for the simulation of suspended sediment in liquid. This is because the associated particle relaxation time is usually much smaller than the time scale in actual flow problems, requiring that a smaller computational time step must be used, which results in considerable computational effort in the numerical time integration. Hence, the single-phase approach is far preferable to the two-phase approach. It should be noted that, although particle drag is absent in the formulation, the single-phase approximation is a two-way coupled approach in which particle drag appears in the form of body force, which is only the case when particles are in the equilibrium state. The other important assumption made in Eqs. (31)–(33) is that the concentration is so small that one can disregard the variation in bulk density as well as the volume occupied by particles. The former condition leads to a single-phase momentum equations under the Boussinesq assumption, while the latter results in incompressibility that is considered only for the continuous phase.

3.3. Case 3: Semi-non-equilibrium approximation

Strictly speaking, it is not always the case that fine particles soon reach the equilibrium state, even if τ_p is very small. In order to see the deviation from the equilibrium state, we define a more general form for the difference in velocity between two phases, $\delta\bar{\mathbf{u}}_{cd}$, as

$$\bar{\mathbf{u}}_d = \bar{\mathbf{u}}_c + \delta\bar{\mathbf{u}}_{cd}. \tag{34}$$

Here, we assume that the inter-phase momentum exchange $\mathbf{M}_{cd}$ is dominated by Stokes drag and the added mass effect, thereby enabling direct application of the final form of the coupled two-phase system (Eq. (20)). Without considering the Reynolds stresses, substituting the relationship given by Eq. (34) into the dispersed-phase momentum equation in Eq. (20) results in

$$\begin{aligned}&\frac{\partial}{\partial t}(\bar{\mathbf{u}}_c + \delta\bar{\mathbf{u}}_{cd}) + (\bar{\mathbf{u}}_c + \delta\bar{\mathbf{u}}_{cd}) \cdot \nabla(\bar{\mathbf{u}}_c + \delta\bar{\mathbf{u}}_{cd}) \\ &\quad = -\left(\mathcal{A}_{(1,1)} - \frac{\phi}{1-\phi} s \mathcal{A}_{(1,2)}\right)\frac{\delta\bar{\mathbf{u}}_{cd}}{\tau_p} - \left(\frac{1}{s}\mathcal{A}_{(1,1)} + \mathcal{A}_{(1,2)}\right)\nabla\bar{p} \\ &\qquad + \mathcal{A}_{(1,1)}\mathbf{g}'.\end{aligned} \tag{35}$$

For a flow-dominant condition in which $\bar{\mathbf{u}}_c \gg \delta\bar{\mathbf{u}}_{cd}$, Eq. (35) can be approximated as

$$\begin{aligned}\frac{\partial \bar{\mathbf{u}}_c}{\partial t} + \bar{\mathbf{u}}_c \cdot \nabla \bar{\mathbf{u}}_c \approx &-\left(\mathcal{A}_{(1,1)} - \frac{\phi}{1-\phi} s \mathcal{A}_{(1,2)}\right)\frac{\delta\bar{\mathbf{u}}_{cd}}{\tau_p} \\ &- \left(\frac{1}{s}\mathcal{A}_{(1,1)} + \mathcal{A}_{(1,2)}\right)\nabla\bar{p} + \mathcal{A}_{(1,1)}\mathbf{g}'.\end{aligned} \tag{36}$$

A further assumption is made by stating that, in a dilute suspension, the continuous phase is not greatly affected by the dispersed phase. Thus, disregarding the Reynolds stresses, the inviscid-flow approximation of Eq. (11) gives the dynamic pressure gradient,

$$-\nabla\bar{p} \approx \frac{\partial \bar{\mathbf{u}}_c}{\partial t} + \bar{\mathbf{u}}_c \cdot \nabla \bar{\mathbf{u}}_c. \tag{37}$$

Substituting Eq. (37) and the corresponding elements of $\mathcal{A}$ into Eq. (36) leads to

$$\left(1 + C_{vm}\frac{\phi}{1-\phi}\right)\left(1 - \frac{1}{s}\right)\frac{D\bar{\mathbf{u}}_c}{Dt} \approx -\frac{\bar{\mathbf{u}}_{cd}}{\tau_p} + \left(1 + C_{vm}\frac{\phi}{1-\phi}\right)\mathbf{g}', \tag{38}$$

where the material derivative $D/Dt = \partial/\partial t + \bar{\mathbf{u}}_c \cdot \nabla$. For dilute suspension, $\phi \approx 0$, Eq. (38) can be further reduced to

$$\delta\bar{\mathbf{u}}_{cd} \approx \tau_p \mathbf{g}' - \tau_p\left(1 - \frac{1}{s}\right)\frac{D\bar{\mathbf{u}}_c}{Dt} \approx w_{s,0}\hat{\mathbf{e}}_3 - \tau_p\left(1 - \frac{1}{s}\right)\frac{D\bar{\mathbf{u}}_c}{Dt}. \tag{39}$$

Eq. (39) describes the evolution of the difference in velocity between two phases as a function of $\tau_p, \mathbf{g}'$, and $D\bar{\mathbf{u}}_c/Dt$, the flow inertia under the condition that $\phi \approx 0$. It can be seen in Eq. (39) that non-equilibrium particle inertia (NEPI) arises from the acceleration of the flow field in the continuous phase. Without acceleration in flow, particles remain in the equilibrium state. This is similar to the simplified EE model derived by Ferry and Balachandar (2001). The simplified EE model has been applied to the study of particle-driven turbidity currents (Cantero et al., 2008; Cantero et al., 2008), in which the motions of particles are described using a formula similar to Eq. (39), and the single-phase incompressible flow solver is used to solve the flow motion, as in Eq. (31). By solving NEPI during the propagation of the turbidity current with different τ_p in a two-dimensional setting, (Cantero et al., 2008) demonstrate the importance of the NEPI in preferential accumulation, an important phenomenon in two-phase dispersed suspension. The formulation in Cantero et al. (2008) slightly differs from the present formulation in which the added mass effect appears in τ_p. One reason for this difference is that Ferry and Balachandar (2001) derive this from the separated dispersed-phase momentum equation disregarding the coupling of the continuous phase, which results in the inclusion of the added mass effect only for particle inertia. However, the final expressions for the velocity difference between two phases are the same.

3.4. Case 4: Hindered settling

In the following, we consider a special case in which particles settle along an infinitely long tube, in which no background flow

field is observed in the continuous phase except for velocities resulting from small amount of feedback force induced by particles. In our domain of interest, the velocity and particle concentration fields are uniform and the system has reached an equilibrium state. This is similar to the experimental setting to determine the hindered settling velocity of fine sediment particles (e.g. Ham and Homsy, 1988), as a means to determine particle size based on the Stokes theorem. Disregarding the Reynolds stress, the coupled two-phase system (Eq. (20)) can be reduced to

$$\mathbf{0} = \mathcal{A}\begin{bmatrix} \frac{\bar{\mathbf{u}}_c - \bar{\mathbf{u}}_d}{\tau_p} + \mathbf{g}' \\ -\frac{\phi}{1-\phi} s \frac{\bar{\mathbf{u}}_c - \bar{\mathbf{u}}_d}{\tau_p} \end{bmatrix} + \mathcal{A}\begin{bmatrix} -\frac{\nabla \bar{p}}{s} \\ -\nabla \bar{p} \end{bmatrix}. \tag{40}$$

Expressing dispersed-phase velocity as the addition of terminal velocity w_s to continuous-phase velocity (i.e. $\bar{\mathbf{u}}_d = \bar{\mathbf{u}}_c + w_s \hat{e}_3$) enables the rearrangement of Eq. (40) as

$$\begin{cases} -\frac{w_s \hat{e}_3}{\tau_p} + \mathbf{g}' = \frac{1}{s}\nabla p \\ \frac{\phi}{1-\phi} s \frac{w_s \hat{e}_3}{\tau_p} = \nabla p, \end{cases} \tag{41}$$

such that the solution for terminal velocity as a function of concentration is easily obtained as

$$w_s = (1-\phi) g' \tau_p = (1-\phi) w_{s,0}, \tag{42}$$

where $w_{s,0} = g'\tau_p$ is the terminal velocity calculated directly from the balance between the gravitational force and Stokes drag. This has been extensively used in the single-phase model. Considering the pressure modulation resulting from the presence of particles, Eq. (41) shows that the use of $w_{s,0}$ as the settling velocity is accurate to $O(1)$ in terms of concentration. It is important to note that the simple expression of Eq. (42) shows that a reduction in the terminal velocity is not related to added mass, which differs from the form of the settling velocity in the study by (Cantero et al., 2008). This is because the present result is derived from a two-way coupled system while (Cantero et al., 2008) considered only the hydrodynamic force on particles without any feedback to the carrier flow. The present result is more precise in the sense that in a uniform and steady flow field, such as in the present case, no added mass effect exists.

As previously mentioned, the present idealized example is similar to the experimental setting used to study the hindered settling of fine particles. In a laboratory setting, fine particles are well mixed and begin settling along a relatively long tube. The speed with which the descending interface between clear water and turbid mixtures develops is examined as a measure of hindered settling velocity of sediment particles. In fact, this settling velocity represents the velocity of the dispersed particle phase, $\mathbf{u}_d$, which has not been determined. In order to obtain hindered settling velocity, we apply incompressibility to the mixture, resulting in the following:

$$\phi \mathbf{u}_d + (1-\phi)\mathbf{u}_c = \text{const.} \tag{43}$$

Because no background velocity exists when $\phi = 0$, we set the constant in Eq. (43) to be zero to obtain $\mathbf{u}_d$ as

$$\mathbf{u}_d = (1-\phi)^2 \mathbf{g}' \tau_p. \tag{44}$$

Eq. (44) provides a first approximation of settling velocity without considering any changes in the rheological properties of sediment–water mixture. Realistically, despite the lack of particulate stress resulting from collisions and friction, there remains a degree of modification in the viscosity of the mixture, which is effective in τ_p (see Eq. (1)) in reducing the settling speed. However, compared to the experimental results of Ham and Homsy (1988), Eq. (44) roughly agrees with the upper bound of the measured settling velocity in the lower concentration range ($\phi < 5\%$), and could therefore serve as a relevant approximation of settling speed in the low concentration range.

4. Deviation from the equilibrium state: A numerical test

Most numerical studies on problems related to fine suspensions employ the single-phase approach; therefore, it is important to investigate the deviation from the equilibrium state. In this section, we perform simple numerical tests of the particle-induced Rayleigh Taylor (RT) instability to quantitatively illustrate how a flow field described by the two-way coupled two-phase simulation deviates from its single-phase approximation. Although the case is very simple, and the resulting flow is laminar, it turns out to be an ideal illustration with which to illustrate the NEPI effect. More complex and realistic examples are presented in the companion study of Chou et al. (submitted for publication).

In the numerical solver, the coupled two-phase system (Eq. (20)) along with Eqs. (4) and (4) are solved through finite-volume discretization. In order to focus on the deviation of the present simulation results from the single-phase approximation, we do not apply any turbulence model for the Reynolds stresses. The solver is originally developed by Zang et al. (1993); Zang et al. (1994) and parallelized by Cui and Street (2001); Cui and Street (2004) to solve the single-phase flow problems. It employs the fractional-step method, in which the predicted velocity field is corrected by the projection of the pressure gradient. The pressure field is solved by enforcing zero divergence to mixture velocity to ensure incompressibility of the sediment–water mixture, i.e. $\nabla \cdot [\phi \bar{\mathbf{u}}_d + (1-\phi)\bar{\mathbf{u}}_d] = 0$.

The numerical simulation is carried out in a three-dimensional domain of size $L \times W \times 2H = 0.015\ \text{m} \times 0.015\ \text{m} \times 0.06\ \text{m}$. The gravitational force acts in the z-direction, the coordinate of which starts from $z = -H$ to H. The grid resolution is $N_x \times N_y \times N_z = 64 \times 64 \times 256$. Simulations are initialized using a particle-containing layer with a volume fraction $\phi_0 = 0.0512$ within the upper half region of the domain and clear water in the lower half. The interfacial instability at $z = 0$ is triggered by an initial perturbation given by

$$\frac{\eta}{L} = \begin{cases} \pm 0.05 \pm 0.05 \cos\left(\frac{\pi r}{\lambda}\right) & \text{if } r < \frac{\lambda}{2} \\ 0 & \text{otherwise,} \end{cases} \tag{45}$$

where $r = \sqrt{(x-x_0)^2 + (y-y_0)^2}$ in which x_0 and y_0 are coordinates of the central point in the horizontal plane, and $\lambda = 0.005$ m. In the top equation of Eq. (45), the positive sign corresponds to a perturbation that generates a rising bubble, while the negative sign corresponds to a falling spike. Domain length L is used as the length scale, such that the time scale T is given by $\sqrt{L/g}$ and the velocity scale is given by $U = \sqrt{Lg}$. Fig. 1 presents images of the concentration contours of a bubble rising in the middle x,z-transect ($y/L = 0.5$) from the two-phase simulation at three time instants. It shows the growth of an initial perturbation forming a mushroom-like rising bubble. This has long been recognized as a typical flow pattern (e.g. Tryggvason and Unverdi, 1990, 1996, 1999) that occurs as lighter fluid penetrates into the upper heavier fluid at the initial stage of the RT instability.

Fig. 2 presents the simulation result in Fig. 1c in conjunction with two different approximations at the same point in time. In the first approximation (Fig. 2b), Eq. (39) is employed to simulate motion of the dispersed phase while motion of the continuous phase is simulated using Eq. (31). It differs from the single-phase approximation in that the model accounts for NEPI in modeling the sediment suspension. However, the feedback to the continuous phase due to NEPI is not considered in this framework. The second approximation applies the single-phase simulation (Fig. 2c) with a

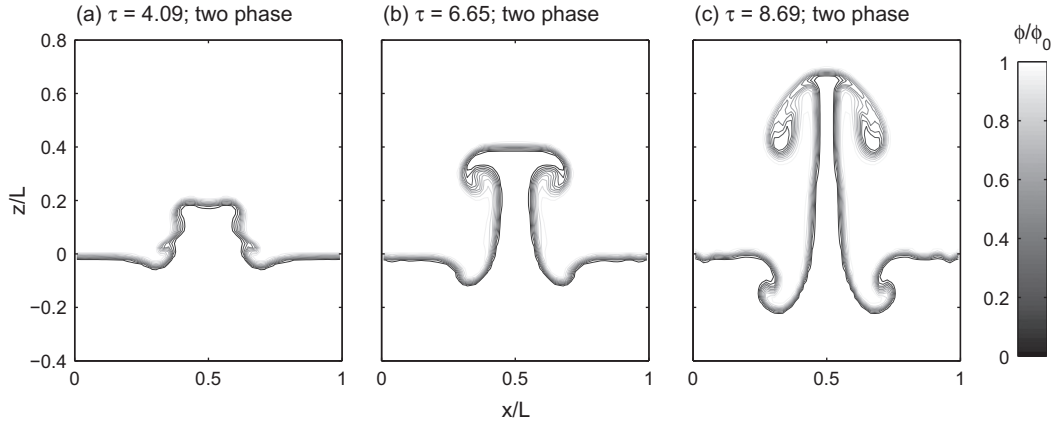

Fig. 1. Normalized concentration contours at the middle x,z-transect $(z/W = 0.5)$ in the domain of a bubble produced from the particle-driven Rayleigh Taylor instability simulated using the present two-phase flow model at τ = (a) 4.09, (b) 6.65, and (c) 8.69.

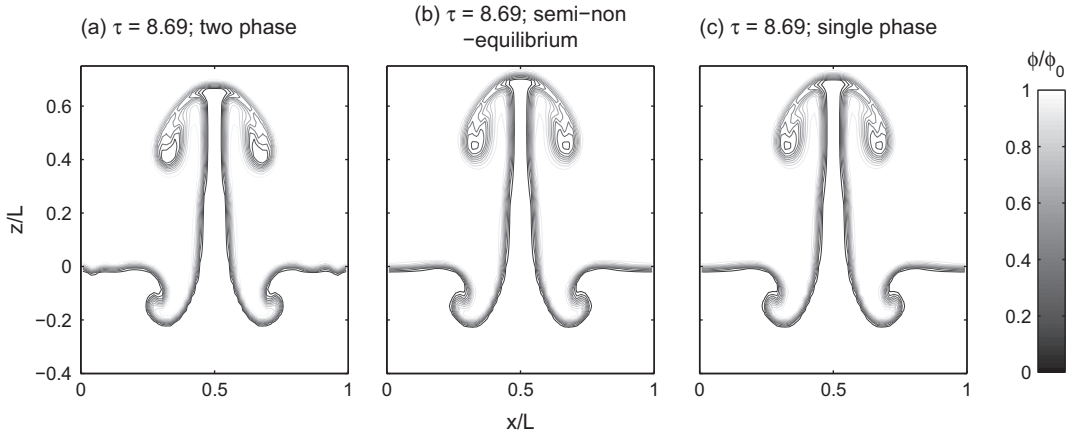

Fig. 2. Normalized concentration contours at the middle x,z-transect $(z/W = 0.5)$ in the domain of a bubble produced from the particle-driven Rayleigh Taylor instability at $\tau = 8.69$ simulated using (a) the present two-phase flow model, (b) the two-phase model without pressure coupling, Eq. (39), and (c) the single-phase model.

constant settling velocity. A comparison of Fig. 2b and c shows that the rising bubble moves with almost the same speed in both cases, which demonstrates that in the present example, NEPI has the negligible effect in motion of the rising bubble. This is because as the low-density clear fluid penetrates into tht high-density turbid fluid to form the rising bubble, the behavior is dominated by the motion of the continuous phase when there is very little entrainment of the turbid fluid into the bubble. A comparison of Fig. 2a and b shows an appreciable decrease of the bubble speed due to NEPI. We can examine how NEPI affects motion of the continuous phase by substituting Eqs. (39) and (26) into Eq. (10) to yield

$$\begin{aligned}\phi_c\rho_c\frac{D\bar{\mathbf{u}}_c}{Dt} &= -\phi_c\rho_c\nabla\bar{p} - \rho_d\phi_d\left(\mathbf{M}'_{cd} - \mathbf{g}'\right) + \nabla\cdot\rho_c\bar{\boldsymbol{\Sigma}}_{vis} \\ &\quad - \rho_d\phi_d\left(1-\frac{1}{s}\right)\frac{D\bar{\mathbf{u}}_c}{Dt} \\ &= \phi_c\rho_c\frac{D\bar{\mathbf{u}}_c}{Dt}\bigg|_{eq} - \rho_d\phi_d\left(1-\frac{1}{s}\right)\frac{D\bar{\mathbf{u}}_c}{Dt}, \end{aligned} \tag{46}$$

where the first term at the RHS of the second identity is the equilibrium-state motion, Eq. (28), which can be calculated using the single-phase method. The last term at the RHS of Eq. (46) is the source/sink term resulting from NEPI, which is a function of local concentration as well as particle and flow properties. It can be seen that if the flow undergoes an upward acceleration $(D\bar{w}_c/Dt > 0)$, there will also be an downward forcing reducing the buoyant force, resulting in a local flow field of the continuous phase that is "heavier" than that of its equilibrium state, despite containing the same amount of sediment. In other words, a downward acceleration in local flow will result in additional upward forcing making the flow "lighter" than that of its equilibrium state. As a consequence, when the flow accelerates, the flow can always be "lagged" by fine particles, depending on local concentrations and particle properties.

5. Summary and conclusion

This study presents a two-way coupled Euler–Euler model for two-phase flow problems involving the suspension of solids. The formulation applies to general two-phase dispersed systems as long as the particle size is small and concentration levels are low. The former condition enables the application of linear drag, while the latter allows the resulting model to disregard particulate stresses. Unlike previous formulations for two-way coupled Euler–Euler systems originally derived from solid–gas systems, the present model includes the effect of added mass, which cannot be overlooked when solid–fluid density ratio is of $O(1)$, as in solid-liquid systems. The inclusion of added mass results in a partition matrix that determines the partitioning of momentum from one phase into the other. The off-diagonal elements in the partition matrix indicate that the coupling effect due to the added mass in the dispersed phase decreases as the density ratio increases; in the continuous phase, the influence of added mass increases with an

increase in local concentration. Therefore, as in a dilute solid–gas system, this can be reduced to a one-way coupled system in which the motion of the dispersed particles are driven by Stokes drag and the body force, while the velocity field of the carrier continuous flow can be obtained by solving the uncoupled single-phase flow equation. An approximation of particles in the equilibrium state can also be derived to yield the single-phase model. By taking into account the non-equilibrium particle inertia (NEPI), a semi non-equilibrium approximation is obtained, illustrating that the difference in velocity between the two phases is a function of the combined effect of the flow inertia and the buoyant force. This gives the same formulation as those reported in previous studies (Ferry and Balachandar, 2001; Cantero et al., 2008; Cantero et al., 2008). An idealized case involving the settling of a uniform concentration of particulate matter in an infinite vertical tube is examined to demonstrate that, with pressure coupling, settling velocity depends on local concentration (i.e. $w_s = (1-\phi)w_{s,0}$), which can be a first-order approximation of the hindered settling velocity in terms of concentration. In order to observe deviations from these approximations, this study presents theoretical analysis as well as simple numerical examples to show the effects of NEPI in individual bubbles arising from the particle-induced Rayleigh–Taylor instability. Because the rising bubble is dominated by the motion of the continuous phase, the present numerical example demonstrates the importance of the feedback from NEPI to the continuous phase.

This paper focuses on the theoretical derivation of a two-way coupled equation applicable to the suspension of fine particles as well as its connection to various approximations often employed in this field. Moreover, the theoretical framework emphasizes the factors that cause the fully coupled two-phase system to deviate from its single-phase approximation. In a companion, Chou et al. (submitted for publication) provides more complex numerical examples on the Rayleigh–Taylor instability.

Acknowledgments

The authors gratefully acknowledge the support of Taiwan NSC Civil and Hydraulic Engineering Program under Grant 101-2218-E-002-004. The research assistantship for WRS was supported by the NSC fund (100-2627-B-002-008) granted to FCW. YJC thanks Oliver Fringer at Stanford University for his extensive suggestions for the development of the present numerical model. The computation is performed on the Dell PowerEdge M620 supercomputer cluster located at Taida Institute of Mathematical Science (TIMS) at National Taiwan University, which is gratefully acknowledged.

References

Amoudry, L., Hsu, T.-J., Liu, L.-F., 2005. Two-phase model for sand transport in sheet flow regime. J. Geophys. Res. 110, C09003.
Auton, T.R., Hunt, J.C.R., Prud'homme, M., 1988. The force exerted on a body in inviscid unsteady non-uniform rotational flow. J. Fluid Mech. 197, 241–257.
Balachandar, S., Eaton, J.K., 2010. Turbulent dispersed multiphase flow. Annu. Rev. Fluid Mech. 42, 111–133.
Bosse, T., Kleiser, L., Meiburg, E., 2006. Small particles in homogeneous turbulence: settling velocity enhancement by two-way coupling. Phys. Fluids 18, 027102.
Cantero, M.I., Garcia, M.H., Balachandar, S., 2008. Effects of particle inertia on depositional particulate gravity currents. Comput. Geosci. 34, 1307–1318.
Cantero, M.I., Balachandar, S., Garcia, M.H., 2008. An Eulerian–Eulerian model for gravity currents driven by intertial particles. Int. J. Multiphase Flow 34, 484–501.
Cantero, M., Balachandar, S., Cantelli, A., Pirmez, C., Parker, G., 2009. Turbidity current with a roof: direct numerical simulation of self-stratified turbulent channel flow driven by suspended sediment. J. Geophys. Res. 114, C03008.
Chen, X., Li, Y., Niu, X., Li, M., Chen, D., Yu, X., 2011. A general two-phase turbulent flow model applied to the study of sediment transport in open channels. Int. J. Multiphase Flow 37, 1099–1108.
Chou, Y.J., Fringer, O.B., 2008. Modeling dilute sediment suspension using large-eddy simulation with a dynamic mixed model. Phys. Fluids 20, 11503.
Chou, Y.J., Fringer, O.B., 2010. A model for the simulation of coupled flow-bed form evolution in turbulent flows. J. Geophys. Res.: Oceans (1978–2012) 115(c10).
Chou, Y.-J., Wu, F.-C., Shih, W.-R., submitted for publication. Toward numerical modeling of fine particle suspension using a two-way coupled Euler–Euler model: Part 2: Simulation of particle-induced Rayleigh–Taylor instability. Int. J. Multiphase Flow.
Cui, A., Street, R.L., 2001. Large-eddy simulation of turbulent rotating convective flow development. J. Fluid Mech. 447, 53–84.
Cui, A., Street, R.L., 2004. Large-eddy simulation of coastal upwelling flow. Environ. Fluid Mech. 4, 197–223.
Dorgan, A.J., Loth, E., 2004. Simulation of particles released near the wall in a turbulent boundary layer. Int. J. Multiphase Flow 30, 649.
Drew, D.A., 1983. Mathematical modeling of two-phase flow. Annu. Rev. Fluid Mech. 15, 261–291.
Drew, D.A., Passman, S.L., 1998. Theory of Multicomonent Fluids. Springer-Verlag, New York.
Elghobashi, S., 1994. On predicting particle-laden turbulent flows. Appl. Sci. Res. 52, 309.
Elghobashi, S., Truesdell, G.C., 1993. On the two-way interaction between homogeneous turbulence and dispersed solid particles. I: Turbulence modification. Phys. Fluids 5, 1790.
Ferry, J., Balachandar, S., 2001. A fast Eulerian method for disperse two-phase flow. Int. J. Multiphase Flow 27, 1199–1226.
Fevrier, P., Simonin, O., Squires, K., 2005. Partitioning of particle velocities in gas–solid turbulent flows into a continuous field and a spatially uncorrelated random distribution: theoretical formalism and numerical study. J. Fluid Mech. 533, 1–46.
Greimann, B.P., Holly Jr., F.M., 2001. Two-phase flow analysis of concentration profiles. J. Hydr. Eng. 127, 753.
Ham, J.M., Homsy, G.M., 1988. Hindered settling and hydrodynamic dispersion in quiescent sedimenting suspensions. Int. J. Multiphase Flow 5, 533–546.
He, X., Zhang, R., Chen, S., Doolen, G., 1999. On the three-dimensional Rayleigh–Taylor instability. Phys. Fluids 11, 1143.
Hsu, T.-J., Jenkins, J.T., Liu, L.-F., 2003. On two-phase sediment transport: dilute flow. J. Geophys. Res. 108, 3057.
Hsu, T.-J., Jenkins, J.T., Liu, L.-F., 2003. On two-phase sediment transport: sheet flow of massive particles. Proc. Roy. Soc. A 460, 2223–2250.
Jha, S.K., Bombardelli, F.A., 2010. Toward two-way flow modeling of nondilute sediment transport in open channels. J. Geophys. Res. 115, F03015.
Li, X.L., Jin, B.X., Glimm, J., 1996. Numerical study of 3D Rayleigh–Taylor instability through the TVE/AC scheme and parallel computation. J. Comput. Phys. 126, 343.
Mulder, T., Syvitski, J.P.M., 1995. Turbidity currents generated at river mouths during exceptional discharge to the world oceans. J. Geol. 103, 285–299.
Necker, F., Hartel, C., Kleiser, L., Meiburg, E., 2002. High-resolution simulations of particle-driven gravity currents. Int. J. Multiphase Flow 28, 279–300.
Necker, F., Hartel, C., Kleiser, L., Meiburg, E., 2006. Mixing and dissipation in particle-driven gravity currents. J. Fluid Mech. 545, 339–372.
Nielsen, P., 1992. Coastal Bottom Boundary Layers and Sediment Transport. World Scientific, Singapore.
Ozdemir, C.E., Hsu, T.-J., Balachandar, S., 2010. A numerical investigation of find particle laden flow in an oscillatory channel: the role of particle-induced density stratification. J. Fluid Mech. 665, 1–45.
Riber, E., Moureau, V., Garcia, M., Poinsot, T., Simonin, O., 2009. Evaluation of numerical strategies for large eddy simulation of particulate two-phase recirculating flows. J. Comput. Phys. 228, 539–564.
Saffman, P.G., 1965. The lift on small sphere in a slow shear flow. J. Fluid Mech. 22, 385–400.
Snyder, P.J., Hsu, T.-J., 2011. A numerical investigation of convective sedimentation. J. Geophys. Res. 116, C09024.
Tryggvason, G., Unverdi, S.O., 1990. Computations of three-dimensional Rayleigh–Taylor instability. Phys. Fluids A 2, 656.
Wang, L.P., Maxey, M.R., 1993. Settling velocity and concentration distribution of heavy particles in homogeneous isotropic turbulence. J. Fluid Mech. 256, 27.
Yang, C.Y., Lei, U., 1998. The role of the turbulent scales in the settling velocity of heavy particles in homogeneous isotropic turbulence. J. Fluid Mech. 371, 179.
Zang, Y., Street, R.L., Koseff, J.R., 1993. A dynamic mixed subgrid-scale model and its application to turbulent recirculating flows. Phys. Fluids A 5, 3186.
Zang, Y., Street, R.L., Koseff, J.R., 1994. A non-staggered grid, fractional step method for time-dependent incompressible Navier–Stokes equations in curvilinear coordinates. J. Comput. Phys. 114, 18.
Zedler, E.A., Street, R.L., 2001. Large-eddy simulation of sediment transport: current over ripples. J. Hydr. Eng. 127, 444.
Zedler, E.A., Street, R.L., 2006. Sediment transport over ripples in sscillatory flow. J. Hydr. Eng. 132, 1.